

Transform spectrometer based on measuring the periodicity of Talbot self-images

Helen L. Kung, Aparna Bhatnagar, and David A. B. Miller

Edward L. Ginzton Laboratory, Stanford University, Stanford, California 94305-4085

Received May 29, 2001

We demonstrate a compact transform spectrometer based on measuring the periodicity of Talbot self-images. The system has no moving parts; it contains only a tilted absorption grating that is imaged onto a CCD camera. The linear architecture of the system makes it possible to use this design in imaging arrays of spectrometers. Unlike other transform spectrometers, its resolution is independent of wavelength. © 2001 Optical Society of America

OCIS codes: 350.0300, 050.0050.

There is a need for compact, inexpensive, nanometer-resolution spectrometers for remote spectral imaging and sensing systems. With *a priori* information on the spectral signature of chemicals or objects, such spectrometers can be used to sense, monitor, and process the spectral content of images. Microelectromechanical systems have made possible many types of small spectrometer, including Fabry–Perot interferometers,¹ grating-based spectrometers,² Michelson spectrometers,³ and standing-wave spectrometers.⁴ Here we demonstrate another method for making a compact transform spectrometer based on measuring the periodicity of Talbot self-images. Unlike typical transform spectrometers, this design has no moving parts, thus increasing reliability while retaining the same fundamental multiplexing advantage of other transform spectrometers. The multiplexing advantage arises because many frequencies of light are present at the detector at all times. This increases the signal-to-noise ratio at the detector. As with other more common transform spectrometers, there is no free spectral range to limit the spectral sensing region. Only the detector response limits the range. Hence this spectrometer may be useful when a large wavelength range is needed in a compact device.

The spectrometer is based on the Talbot effect, first observed by H. F. Talbot in 1836.⁵ The Talbot effect occurs when a spatially periodic object such as a grating is illuminated with spatially coherent light. A series of self-images, replicas of the spatially periodic object, occur in the longitudinal direction (z) parallel to the grating because of Fresnel diffraction. The location of the self-images is periodic, with a spacing of⁶

$$\Delta z = \frac{\lambda}{1 - [\lambda^2/\Lambda^2]^{1/2}}, \quad (1)$$

where λ is the wavelength and Λ is the period of the spatially periodic object. When the diffraction angle is small ($\lambda \ll \Lambda$), Δz is approximately $2\Lambda^2/\lambda$. Equally spaced but interleaved with the self-images are reversal images, in which the light and dark regions of the light field pattern are reversed.

The generation of self-images can be explained by consideration of the diffraction orders of the grating.

Each diffraction order contains a spatial frequency component of the grating. Perfect self-images occur at those locations where the diffraction orders add in phase. Reversal images occur where the diffraction orders add out of phase.⁶ Beyond a distance z_{\max} from the grating, there is no longer overlap of any of the diffraction orders. This distance is given by

$$z_{\max} = \frac{W}{2} [\Lambda^2/\lambda^2 - 1]^{1/2} \approx W\Lambda/2\lambda, \quad (2)$$

where W is the width of the beam or the grating size, whichever is smaller.

Lohmann⁷ proposed the first type of Fourier-transform (FT) spectrometer based on the Talbot effect in 1961. Since the spacing of the Talbot self-image planes has a longitudinal periodicity that is approximately proportional to $1/\lambda$, one can determine the optical spectrum by measuring the periodicity of the self-images. For different wavelengths the Talbot self-images are located at different planes. Each wavelength has its own Talbot image location and reversal location. The total intensity at a given point is the sum of the intensities of each wavelength present in the spectrum considered individually. The assumptions described above are valid only when the grating is not subwavelength. By taking the FT with respect to distance (z), one can determine the spectrum of the input signal.

Measuring the periodicity of the Talbot self-images without moving parts requires multiple detectors. In our approach, Talbot self-images were generated by a grating rotated about an axis perpendicular to the grating lines and to the incident beam (see the bottom of Fig. 1). The edge of the grating closest to a CCD was imaged and magnified onto the CCD with a lens. The lens was necessary for magnification because the grating lines were smaller than the pixel size of the CCD. Without magnification, more than one line would be imaged onto the CCD, and one would not be able to tell the difference between reversal and image planes, which would reduce the ability of the system to resolve the Talbot effect. The object plane of the lens system is the plane that is normal to the incident light and contains the closest edge of the grating.

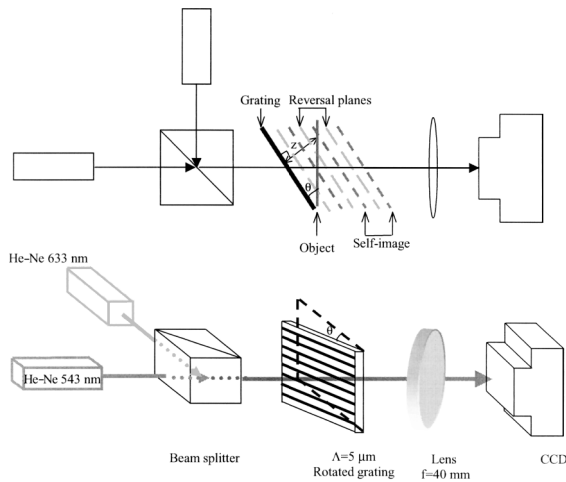


Fig. 1. Optical setup: top, top view of the setup; bottom, three-dimensional view of the setup. Two different He-Ne laser beams are combined with a beam splitter and are made collinear with each other. The light then passes through a rotated grating and is imaged with a 40-mm focal-length lens onto a CCD camera. From the three-dimensional view, note that the grating is rotated about an axis perpendicular to the horizontal grating lines. The top view shows the Talbot-self-image planes behind the grating. The distance z is the perpendicular distance from the grating to the object plane of the lens. θ is the angle of rotation from normal incidence.

The top view of the optical setup in Fig. 1 shows the location of the Talbot planes behind the grating and the location of the object plane. If the distance from the grating to the object plane is a Talbot multiple, then there is a true image on the CCD. If the distance is a Talbot reverse-image multiple, then a reversed image appears on the CCD. By feeding the output of a single horizontal row of the CCD into an oscilloscope and taking the FT, we can measure the periodicity of the Talbot planes, thus determining the spectrum. Since only one row of the CCD was used, the CCD could have been replaced with a one-dimensional detector array.

In the optical setup shown in Fig. 1, green (543-nm) and red (633-nm) He-Ne lasers are collinearly combined with a beam splitter. An amplitude transmission grating rotated at an angle of $\theta = 52^\circ$ was used to generate the Talbot self-images. A 40-mm focal-length lens was used to image the closest edge of the grating onto a CCD camera of width 6.55 mm and height 4.87 mm. The grating was magnified ~ 4.9 times. The FWHM of the red laser spot was 2.0 mm, with a power of $345 \mu\text{W}$. The green laser had a FWHM of 1.5 mm and a power of $312 \mu\text{W}$. The grating was rotated so that its horizontal lines were parallel to the horizontal line scan of the CCD camera. The CCD camera had a neutral-density filter in front of it that attenuated 99.1% of the light.

The only nonstandard component used in this experiment was the absorption grating. It was fabricated first by evaporation of 100 nm of aluminum onto a 100-cm-diameter quartz wafer. The wafer was then patterned so that alternating aluminum lines with spaces of equal width $\Lambda/2$, where $\Lambda = 5 \mu\text{m}$,

were left. The total area of the grating was 6 mm by 6 mm.

We demonstrated the use of this system as a spectrometer as follows: The intensity profile was read horizontally across 512 pixels of the CCD, ac coupled, and Fourier transformed. The untransformed intensity for each single wavelength is shown in Fig. 2. As shown in the graph, there is an oscillation in the intensity across the row of the CCD. The oscillation period is proportional to that of the Talbot period. The period of the fringes is larger for green than for red. This result shows that, if one knows the fringe spacing, it is possible to determine the spectrum. The trace for simultaneous red and green illumination is shown in Fig. 3. The expected beat frequency is visible from the curves. The FTs of the red data, the green data, and the data when both lasers are on are shown in Fig. 4. For the case in which both lasers are on, the FT plot shows two clearly resolved peaks that correlate well with the peaks from only the red or the green laser. This correlation demonstrates the utility of this setup for spectrometry. Using the wavelength for red light (633 nm) for calibration, we find that the green (543-nm) peak has a Talbot period of $91.8 \mu\text{m}$, as expected from Eq. (1). The FWHM of the FT peak is 48 nm.

The method of determining resolution for this spectrometer is similar to that for any other transform

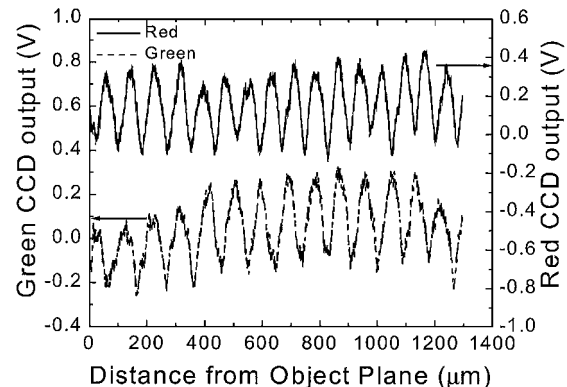


Fig. 2. ac-coupled output of one row of the CCD camera when either the red or the green laser is shining into the spectrometer.

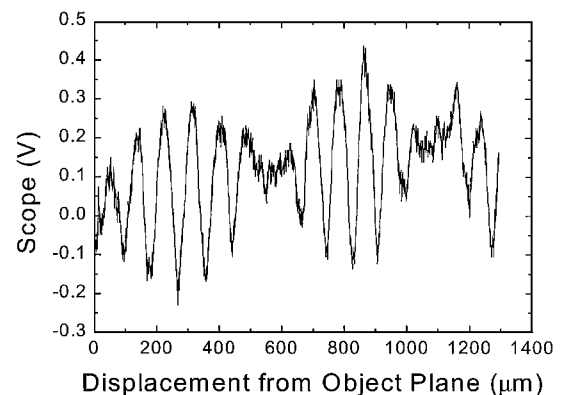


Fig. 3. ac-coupled output of one row of the CCD camera with both the red and the green lasers simultaneously shining into the spectrometer.

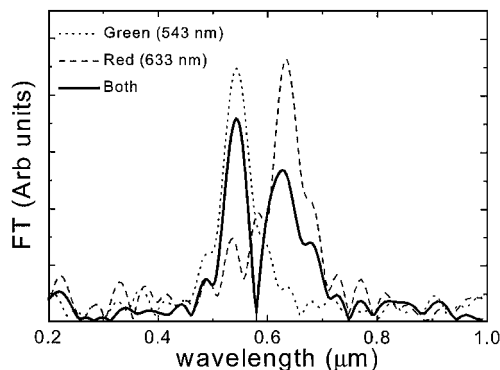


Fig. 4. FTs of red, green, and both lasers. The frequency axis was converted to the corresponding wavelength.

spectrometer. The conservative criterion for resolving two wavelengths, λ_1 and λ_2 , is having one more period at λ_1 than at λ_2 . The number of planes seen by the CCD depends on the tilt of the grating (θ), the wavelength of light (λ), the period of the grating (Λ), the magnification (M) of the lens, the beam size (W), and the size of the CCD (L), according to the following equation:

$$\text{Number of Talbot planes} = \frac{\lambda L \sin \theta}{2M\Lambda^2}. \quad (3)$$

Equation (3) is valid only if Talbot self-images exist in the entire image plane detected by the CCD. This condition is satisfied by

$$\frac{W}{2} \left[\left(\frac{\Lambda}{\lambda} \right)^2 - 1 \right] \geq \frac{L \sin \theta}{M}. \quad (4)$$

In this regime the resolution criterion implies that

$$\Delta\lambda = |\lambda_1 - \lambda_2| = \frac{2M\Lambda^2}{L \sin \theta}. \quad (5)$$

For our given grating, magnification, and rotation, the best resolution is 42 nm. The difference between this resolution and the FWHM of our FT peak could be due to a small inaccuracy of the measurement of the magnification or grating angle. The resolution of this spectrometer increases quadratically with decreasing

grating pitch; thus using a grating with a finer period will improve the resolution. One interesting point to note is that the resolution is not dependent on wavelength. Thus the wavelength resolution of this type of spectrometer is equally good at longer or shorter wavelengths, which might be an advantage over other transform spectrometers.

In conclusion, we have demonstrated a transform spectrometer based on measuring the location of Talbot self-image planes. It requires no moving parts, and the spectral range is dependent only on the detector's response curve. This particular design needs only a one-dimensional array of detectors. The spectrometer has a linear architecture, so it is possible to fabricate arrays of Talbot spectrometers for imaging applications. This particular spectrometer's resolution was limited by the grating period. The Talbot spectrometer's wavelength resolution is not dependent on the wavelength. Future improvements will include implementation of a smaller grating pitch and integration of the grating, lens, and detector array.

We acknowledge stimulating discussions with David M. Bloom and Joseph W. Goodman on using the Talbot effect as a method of making a transform spectrometer. This work was supported by contract MDA972-98-1-0002 from the Defense Advanced Research Projects Agency, a subaward from the University of New Mexico. H. L. Kung was supported by a Lucent Technologies Graduate Research Program for Women grant. A. Bhatnagar was supported by a Herb and Jane Dwight Stanford Graduate Fellowship. H. L. Kung's e-mail address is hlkung@stanford.edu.

References

1. P. M. Zavracky, K. L. Denis, H. K. Xie, T. Wester, and P. Kelley, *Proc. SPIE* **3514**, 179 (1998).
2. G. M. Yee, N. I. Maluf, P. A. Hing, M. Albin, and G. T. A. Kovacs, *Sens. Actuators A* **58**, 61 (1997).
3. O. Manzardo, H. P. Herzig, C. R. Marxer, and N. F. de Rooij, *Opt. Lett.* **24**, 1705 (1999).
4. H. L. Kung, S. R. Bhalotra, J. D. Mansell, and D. A. B. Miller, in *International Conference on Optical MEMS* (Institute of Electrical and Electronics Engineers, New York, 2000), pp. 19–20.
5. H. F. Talbot, *Philos. Mag.* **9**, 401 (1836).
6. R. F. Edgar, *Opt. Acta* **16**, 281 (1969).
7. A. W. Lohmann, in *Proceedings of the Conference on Optical Instruments and Techniques, London* (Wiley, New York, 1961), p. 58.